

Tunable Optical and Swelling/Deswelling Properties Associated with Control of the Coil-to-Globule Transition of Poly(*N*-isopropylacrylamide) in Polymer–Clay Nanocomposite Gels

Kazutoshi Haraguchi,^{*,†} Huan-Jun Li,[†] Liyuan Song,[‡] and Kazutaka Murata[†]

Material Chemistry Laboratory, Kawamura Institute of Chemical Research, 631 Sakado, Sakura, Chiba 285-0078, Japan, and College of Material Science and Engineering, Donghua University, Shanghai 200051, China

Received June 18, 2007; Revised Manuscript Received July 13, 2007

ABSTRACT: Polymer–clay nanocomposite gels (NC gels) consisting of poly(*N*-isopropylacrylamide) (PNIPA) and inorganic clay (hectorite) were investigated in terms of their optical and swelling/deswelling properties. Depending on the clay concentration (C_{clay}), NC gels exhibit unique changes in optical transmittance, optical anisotropy, and swelling/deswelling behaviors, all of which were distinct from those of chemically cross-linked hydrogels (OR gels). The optical transparency and its temperature-induced change differed greatly between NC and OR gels. The decrease in transmittance associated with the coil-to-globule transition of PNIPA occurred at higher temperatures than the normal transition temperature in NC gels as the clay concentration increased. On the assumption of the uniform and random dispersion of exfoliated clay platelets, the critical C_{clay} (C_{clay}^*) for spontaneous clay aggregation (layer stacking) in NC gels was calculated to be 10×10^{-2} mol/L H_2O . C_{clay}^* was consistent with the experimental results, including the mechanical properties of strength and modulus, the transparency changes induced by temperature, and the appearance of optical anisotropy. Optical anisotropy was observed in NC gels with clay concentrations above C_{clay}^* , and by increasing the water content, it could be reversibly changed to isotropy when C_{clay} was close to C_{clay}^* . The swelling of NC gels at 20 °C and their deswelling at 50 °C were both depressed greatly with increasing C_{clay} . Furthermore, NC gels with C_{clay} higher than that of NC12 gel exhibited swelling even at 50 °C, and it is expected that NC gels whose volume remains unchanged regardless of temperature can be produced by further increasing C_{clay} . All of these unique changes in the properties of NC gels can be explained by the partial phase separation due to the coil-to-globule transition of PNIPA and the dispersion morphology of clay platelets.

Introduction

Since Heskins and Guillet¹ found that poly(*N*-isopropylacrylamide) (PNIPA) exhibits a well-defined coil-to-globule transition at a lower critical solution temperature (LCST) in aqueous media, PNIPA and its hydrogels have been extensively studied in terms of the mechanism of phase transition,² the role of hydrophobic effects in aqueous media (e.g., the formation of a water cage around the isopropyl group³), the external stimuli bringing about the transition (e.g., temperature,⁴ pH,⁵ magnetic field,⁶ pressure,⁷ salt,⁸ solvent^{2a,4a}), and many promising applications in the form of stimulus-sensitive soft materials (e.g., drug-delivery systems,⁹ artificial actuators,¹⁰ colloid crystals,¹¹ separation devices,¹² and tissue engineering¹³). Concurrently, constant efforts have been made to control the stimulus sensitivity of PNIPA hydrogels by shifting the LCST from the usual value (≈ 32 °C),^{2a} altering the volume ratio of swelling/deswelling,¹⁴ and accelerating the deswelling rate at temperatures above LCST,¹⁵ in addition to improving their very weak and brittle mechanical properties.¹⁶ However, so far, those trials have been mostly carried out using chemically cross-linked PNIPA hydrogels prepared with an organic cross-linker. Consequently, the resulting controls and improvements have been hardly appropriate for real applications because the fragile nature of PNIPA hydrogels have remained essentially unchanged and the problem has been shelved.

We have recently found that novel nanocomposite-type hydrogels (“NC gels”) with a unique organic (polymer)/inorganic (clay) network structure can simultaneously solve all of the problems associated with chemically cross-linked hydrogels (“OR gels”), including their mechanical fragility.¹⁷ NC gels composed of PNIPA, hydrophilic inorganic clay, and water exhibited excellent optical and swelling/deswelling properties as well as extraordinary mechanical properties compared with those of conventional PNIPA–OR gels.¹⁸ These characteristics were mainly attributed to the organic/inorganic network structure in which exfoliated clay platelets, uniformly dispersed on a nanometer scale, act as multifunctional cross-linking units whereby a large number of polymer chains are attached to the clay platelet surfaces forming a plane of cross-linking points.¹⁹ In a previous communication,²⁰ we reported that ultrahigh mechanical properties and total control of the coil-to-globule transition of PNIPA chains became possible in NC gels with high clay concentrations. In a subsequent paper,²¹ we revealed the effect of high clay contents on the mechanical properties of PNIPA–NC gels in detail, such as the possibility of extensively controlling the tensile strength, which reached 1 MPa in the as-prepared state and 3 MPa after an elongation treatment, the highly reversible extensibility of around 1000%, the time-dependent recovery from elongation, the similar possibility of controlling the compressive mechanical properties, the appearance of optical anisotropy depending on the clay concentration, etc. In the present paper, we report the highly tunable optical and swelling/deswelling properties of (PNIPA–) NC gels with a broad range of clay contents.

* Corresponding author: e-mail: hara@kicr.or.jp; Fax (+81) 43-498-2182; Tel (+81) 43-498-2111.

[†] Kawamura Institute of Chemical Research.

[‡] Donghua University.

Basically, the coil-to-globule transition of PNIPA is a phenomenon occurring in very dilute solution. However, in semidiluted systems (such as the present NC gels), the changes in transmittance (turbidity) and swelling/deswelling of the hydrogel occur by partial phase separation arising from the same phenomenon (coil-to-globule transition) in cross-linked PNIPA chains. Then, in the following discussion, the term coil-to-globule transition is used as the description for such changes in PNIPA hydrogels.

Experimental Section

Raw Materials. *N*-Isopropylacrylamide (NIPA), provided by Kohjin Co., Japan, was purified by recrystallization from a toluene/*n*-hexane mixture (2/1 w/w) and dried under vacuum at 40 °C. *N,N*-Dimethylacrylamide (DMAA) monomer, provided by Kohjin Co., Japan, was purified by filtering through activated alumina. Other reagents were purchased from Wako Pure Chemical Industries, Japan, and used without further purification. The water used for all experiments was ultrapure water supplied by a Puric-Mx system (Organo Co., Japan). Dissolved oxygen in the pure water was removed by bubbling nitrogen gas for more than 3 h prior to use, and throughout all experiments, oxygen was excluded from the system. As the inorganic clay, the synthetic hectorite "Laponite XLG" (Rockwood, Ltd., UK; $[\text{Mg}_{5.34}\text{Li}_{0.66}\text{Si}_8\text{O}_{20}(\text{OH})_4]\text{Na}_{0.66}$; layer size = 30 nm diameter \times 1 nm thickness;²² cation exchange capacity = 104 mequiv/100 g) was used after washing and freeze-drying. Here, we used the molar mass based on the unit chemical composition as the molar mass of Laponite XLG: 762 g/mol. Potassium persulfate (KPS) and *N,N,N',N'*-tetramethylethylenediamine (TEMED) were used as the initiator and the catalyst, respectively.

Synthesis of PNIPA Hydrogels. Uniform aqueous solutions containing clay at concentrations of 1×10^{-2} – 20×10^{-2} mol/L of H_2O , and monomer at a constant concentration of 1 mol/L of H_2O , were prepared. The clay content in NC gel, C_{clay} , was expressed using a simplified numerical value of 1–20 corresponding to the clay concentration in the initial reaction solution described above. Also, the PNIPA–NC gels were simply named NC1 gel, NC20 gel, etc., without using PNIPA as prefix, according to the C_{clay} (1–20). The synthesis procedures for the NC gels with low and high C_{clay} were the same as those reported previously.^{17,18,20,21} As a typical example, to prepare the NC5 gel, a transparent aqueous solution consisting of water (19 mL), inorganic clay (0.762 g), and NIPA (2.26 g) was prepared. Next, the catalyst (TEMED, 16 μL) and, finally, an aqueous solution of the initiator (0.02 g of KPS in 1.0 mL of H_2O) were added to the former solution at iced-water temperature while stirring. The amount of clay was varied from 0.152 g (NC1) to 3.05 g (NC20). The molar ratio of the monomer (NIPA), initiator (KPS), and catalyst (TEMED) was fixed at 100:0.426:0.735. Then, in-situ free-radical polymerization was allowed to proceed in a water bath at 20 °C for 20 h. By using a similar procedure, DMAA–NC gels (D–NC gels) with different clay concentrations (D-NC1–D-NC10) were prepared. Meanwhile, PNIPA–OR gels were prepared using NIPA (2.26 g, 1 mol L⁻¹ in H_2O) and an organic cross-linker (*N,N'*-methylenebis(acrylamide)) (BIS) at a concentration of 1–10 mol % (0.028–0.280 g) relative to NIPA. The PNIPA–OR gels were simply named OR1 gel–OR10 gel according to the BIS concentration (C_{BIS}). Linear polymer PNIPA (LR) was prepared similarly but using no cross-linking agent. For the calculation of the clay/PNIPA ratio by volume, the densities of 2.65 and 1.10 g/cm³ were used for the clay²³ and PNIPA,²⁴ respectively.

Measurements. *Optical Transmittance.* Optical transmittances were measured at 600 nm using a UV–vis spectrophotometer (V-530, Jasco Corp., Japan) equipped with a thermostatic cell (VT-100, Jasco Corp.) for NC gels, D–NC gels, and LR, all of which were prepared in a cubic polystyrene cuvette (10 \times 10 \times 44 mm in length) with a cap. Changes in optical transmittance induced by increasing the temperature from 20 to 50 °C were measured at a heating rate of 0.167 °C/min. Ultrapure water was used as the reference.

Optical Anisotropy. Optical anisotropy was observed for NC gels with a thickness of 2 mm and diameter of 25 mm, which were cut from cylindrical gels and were examined by means of a polarizing microscope (Nikon, Eclipse LV100 Pol) with crossed polarizers. Birefringences ($\Delta n = \Gamma$ (retardation)/ d (thickness)) of NC gels were determined using Berek and Senarmont compensators in conjunction with crossed polarizers.

Swelling and Deswelling Ratios. Swelling and deswelling experiments were performed by immersing the as-prepared NC and OR gels (initial size 5.5 mm diameter \times 30 mm length) in a large excess of water at 20 and 50 °C, respectively, for \sim 200 h, changing the water several times. Throughout the experiments, the weight of the gel was measured at specific times after removing excess water from the surface. Swelling and deswelling ratios were represented by the ratio of the weight of the water in the hydrogel to that of the corresponding dried gel ($W_{\text{H}_2\text{O}}/W_{\text{dry}}$) or by the ratio of the weight of the hydrogel to the corresponding as-prepared gel (W_{gel}/W_0). Here, $W_{\text{H}_2\text{O}} = W_{\text{gel}} - W_{\text{dry}}$. In order to determine the repeated swelling/deswelling behavior, as-prepared NC1, NC5, NC10, and NC20 gels of the same size were kept in water alternatively at 50 °C for 48 h and at 20 °C for 48 h. The change in gel weight was represented by $W_{\text{gel}}(t)/W_{50}(48)$, where $W_{\text{gel}}(t)$ is the gel weight at the specific time t (h), and $W_{50}(48)$ is the gel weight after submersion for the first 48 h at 50 °C.

Results and Discussion

Transparency Changes in the NC and OR Gels across the LCST. As reported in previous papers,^{20,21} uniform and transparent NC gels were obtained almost regardless of C_{clay} . Also, all NC gels were mechanically very tough and exhibited characteristic changes in tensile modulus (\sim 500 kPa), strength (\sim 1000 kPa), and fracture energy (up to 3300 times that of OR gels) depending on C_{clay} , in addition to the unchanged high elongation at fracture (about 1000%). In contrast, OR gels as produced were opaque when C_{BIS} was above OR5, and all OR gels exhibited very weak mechanical properties regardless of C_{BIS} . In this paper, we first describe changes in the optical transparencies of NC and OR gels with different cross-linker contents induced by altering the temperature across the LCST. Panels a-1 and a-2 of Figure 1 show the transparencies of the NC3 and NC15 gels measured at 20 °C (<LCST) and 50 °C (>LCST), respectively. The NC3 gel showed a peculiar change from transparent to opaque due to the coil-to-globule transition of PNIPA, but the NC15 gel did not undergo any change in transparency, retaining its high transparency even at 50 °C. For comparison, changes in the transparency of the OR1 and OR5 gels are shown in panels b-1 and b-2 of Figure 1. Because of the frozen network inhomogeneity caused during the course of polymerization and cross-linking, the transparencies of as-prepared OR gels decreased significantly with increasing C_{BIS} . Thus, OR5 gel was opaque in the as-prepared state at 20 °C. At 50 °C, both the OR1 gel and the OR5 gel were opaque. Thus, the transparencies of PNIPA hydrogels, prepared using different cross-linkers, clay and BIS, showed different changes with temperature, depending on the kind of network structure and the concentration of each cross-linker. Also, the results shown in Figure 1(a-1) indicate that a uniform organic (PNIPA)/inorganic (clay) network structure was retained in all NC gels regardless of C_{clay} , while network inhomogeneity was remarkably enhanced in the OR gel with a high C_{BIS} (Figure 1(b-1)).

Temperature Dependence of the Optical Transmittance of NC Gels. The details of changes in optical transmittance induced by increasing the temperatures of NC gels with different C_{clay} (NC3–NC15) and a viscous solution of linear PNIPA (LR: NC0) are shown in Figure 2a. Here, the transmittance at 600 nm was measured as a function of temperature, which was

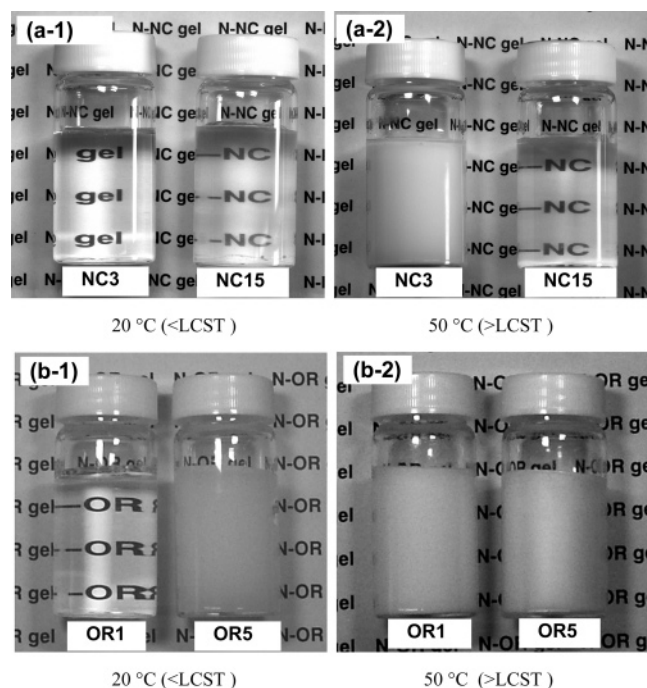


Figure 1. Photographs depicting changes in transparency for (a) NC3 and NC15 gels and (b) OR1 and OR5 gels at 20 °C (<LCST) and 50 °C (>LCST), respectively.

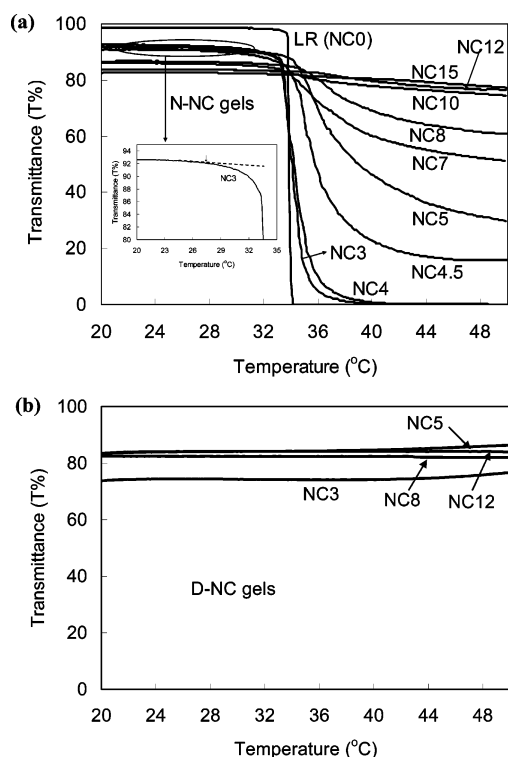


Figure 2. Transmittance changes with temperature in (a) NC gels and (b) D-NC gels with different C_{clay} (NC0–NC15 gels). Wavelength is 600 nm. Heating rate: 0.167 °C/min. The thicknesses of NC and D-NC gels are 10 mm.

slowly increased at a rate of 0.167 °C/min. As shown in Figure 2a, NC gels with lower C_{clay} (\leq NC4) exhibited a sharp change in transmittance at around 34 °C, a temperature corresponding to the LCST, similar to that of LR (NC0). On the other hand, for NC gels with high C_{clay} (\geq NC4), the transition temperature range gradually broadened, particularly at higher temperatures. The optical transmittance at 50 °C increased steeply with increasing C_{clay} , and the apparent LCST, defined as the

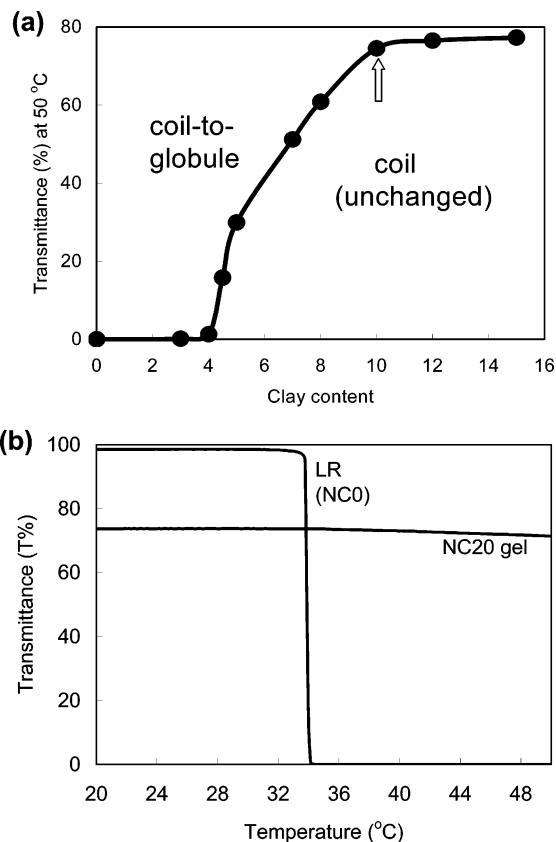


Figure 3. (a) C_{clay} dependence of the transmittance (600 nm) in NC gels measured at 50 °C. The arrow indicates the critical clay concentration, above which the transmittance change is hardly observed. (b) Temperature–transmittance relationship of the NC20 gel and that of a linear PNIPA solution.

temperature at which the transparency had decreased by 50% of the total decrease in the range of 20–50 °C, gradually shifted to a high temperature: 34.2 °C for NC3, 36 °C for NC4.5, and 37.5 °C for NC5. Furthermore, the loss of transmittance at 50 °C, which corresponds to PNIPA in which phase separation (i.e., coil-to-globule transition) had occurred, dramatically decreased with increasing C_{clay} , particularly in the range of NC4–NC10, as shown in Figure 3a. Consequently, it was concluded that there is a critical C_{clay} ($\approx 10 \times 10^{-2}$ mol/L H_2O), above which NC gels exhibit hardly any change in transmittance if the temperature is altered: as shown in Figure 3b, totally different temperature–transmittance relationships were found in the PNIPA aqueous systems LR (NC0) and NC20 gel, the latter containing inorganic clay nanoparticles.

On the contrary, in D-NC gels consisting of the non-thermally sensitive polymer (PDMAA), there was no well-defined decrease in transparency when the temperature was increased, regardless of C_{clay} , as shown in Figure 2b. Therefore, the remarkable changes (decreases) in transmittance observed in NC gels (Figure 2a) should be related to the thermally sensitive coil-to-globule transition of PNIPA. Thus, the temperature-induced changes in transmittance of NC gels varied greatly, in both magnitude (decrease) and temperature (to higher temperatures), as a result of incorporating inorganic clay nanoparticles. This effect may be attributed to restrictions in thermal motions of PNIPA chains attached to the hydrophilic clay surfaces or in their proximity. As described later in this paper, the clay platelets tended to form a kind of regular stacking (the origin of optical anisotropy) in NC gels with increasing C_{clay} . In between a number of exfoliated clay platelets with a relatively small interlayer distance, the thermally triggered

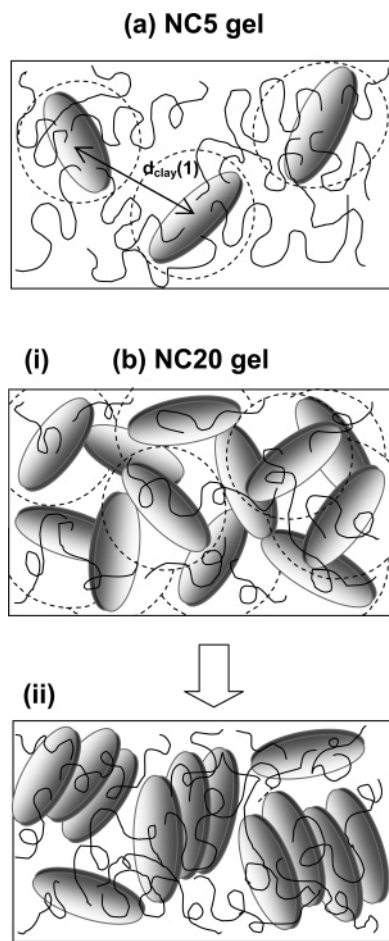


Figure 4. Schematic representation of the structural models for NC gels: (a) for NC5 gel, with a uniform and random dispersion of clay platelets; (b) for NC20 gel; (i) a uniform and random dispersion of clay platelets and (ii) spontaneous aggregation (layer stacking) of clay platelets.

conformational change in the PNIPA chains from hydrated (coil) to dehydrated (globular) state, which corresponds to the dissociation of the hydration shell in the water cages around the hydrophobic *N*-isopropyl groups,³ was hindered and/or occurred at elevated temperatures, probably due to the predominantly hydrophilic circumstances and/or steric hindrances at the periphery of the clay platelets.

More precisely, as shown in the inset of Figure 2, the optical transmittance of NC3 gel started to decrease slightly at low temperature (ca. 27 °C). A similar decrease in transmittance at low temperature was also observed in other NC gels, such as NC1–NC4. These results suggest that the coil-to-globule transition in N–NC gels occurs across a broad temperature range, at high temperature in major parts of the gels, but at low temperature in small parts of the gel. The reason for the occurrence of coil-to-globule transition at lower temperature has not been elucidated yet. This phenomenon will be discussed in a subsequent paper by comparing data with those of OR gels. However, it is important to note that, although the thermally triggered coil-to-globule transition of PNIPA was greatly hindered by their interaction with clay platelets as C_{clay} increased (Figure 2a), the large deformability of 900–1300% in uniaxial stretching was observed for all NC gels with different C_{clay} ,^{20,21} which indicates that PNIPA chains still adopted random conformations even in NC gels with high C_{clay} .

Dispersion Morphology of the Clay Platelets in NC Gels. Assuming a uniform, random dispersion of exfoliated clay platelets, with a diameter of 30 nm and a thickness of 1 nm, the average inter-clay–platelet distance, $d_{\text{clay}}(1)$, in the NC gels

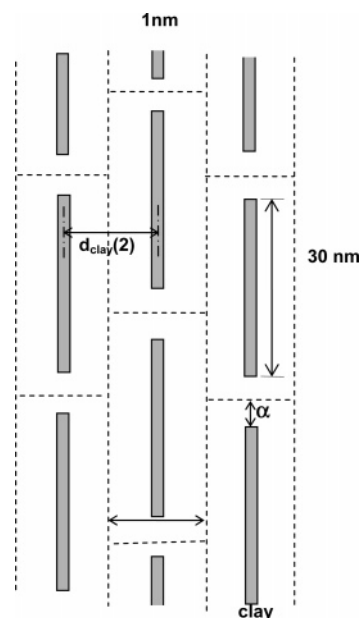


Figure 5. Schematic representation of the structural models with the uniform and unidirectional alignment of clay platelets for NC gels with $C_{\text{clay}} \gg C_{\text{clay}}^{\text{crit}}$.

was calculated from eq 1 to be 38.01, 30.30, and 24.25 nm for the NC5, NC10, and NC20 gels, respectively:

$$d_{\text{clay}}(1) = \left(\frac{V_{\text{clay}} \hat{\rho}_{\text{clay}}}{m_{\text{clay}} C_{\text{clay}} q} \right)^{1/3} \quad (1)$$

where

$$q = \frac{1000}{1000 + (m_{\text{NIPA}} C_{\text{NIPA}} / \hat{\rho}_{\text{PNIPA}}) + (m_{\text{clay}} C_{\text{clay}} / \hat{\rho}_{\text{clay}})}$$

and V_{clay} , $\hat{\rho}_{\text{clay}}$ ($\hat{\rho}_{\text{PNIPA}}$), and m_{clay} (m_{PNIPA}) are the volume, the mass density, and the monomer-equivalent molar mass of clay platelets (PNIPA), respectively. Also, q is close to 1 when C_{clay} is small and $C_{\text{NIPA}} = 1$ M. Since $d_{\text{clay}}(1)$ for NC5 gel (38.01 nm) was larger than the diameter of the clay platelet (30 nm), the clay platelets were free to adopt all orientations without restriction by their neighbors (Figure 4a). In contrast, in NC20 gel, clay platelets presumably aggregated (became stacked) spontaneously to some degree in the as-prepared state (without elongation) because $d_{\text{clay}}(1)$ was small (24.25 nm), as shown in Figure 4b, (i) \rightarrow (ii). The critical C_{clay} , C_{clay}^* , at which $d_{\text{clay}}(1)$ is the same as the clay diameter, corresponded to NC10 ($d_{\text{clay}}(1) = 30.30$ nm). These results are consistent with the results reported in the previous paper.²¹ That is, optical anisotropy was observed in as-prepared NC gels with C_{clay} above that for NC10, while no (or pronounced) optical anisotropy was observed in the as-prepared NC5 (or NC20) gel. Also, C_{clay}^* calculated here (NC10) is the same as both the critical C_{clay} obtained as a result of the changes in tensile mechanical properties (strength and modulus)²¹ and the critical C_{clay} for the hindrance of the coil-to-globule transition described above (Figure 3a).

Next, assuming a uniform and unidirectional alignment (quasi-nematic structure) of the clay platelets shown in Figure 5, the average inter-clay–platelet distance, $d_{\text{clay}}(2)$, was calculated using eq 2:

$$d_{\text{clay}}(2) = \frac{V_{\text{gel}}}{(30 + 2\alpha)^2} \left(\frac{V_{\text{clay}} \hat{\rho}_{\text{clay}}}{m_{\text{clay}} C_{\text{clay}} q} \right) \quad (2)$$

Here, the structural unit consisting of a clay platelet and its

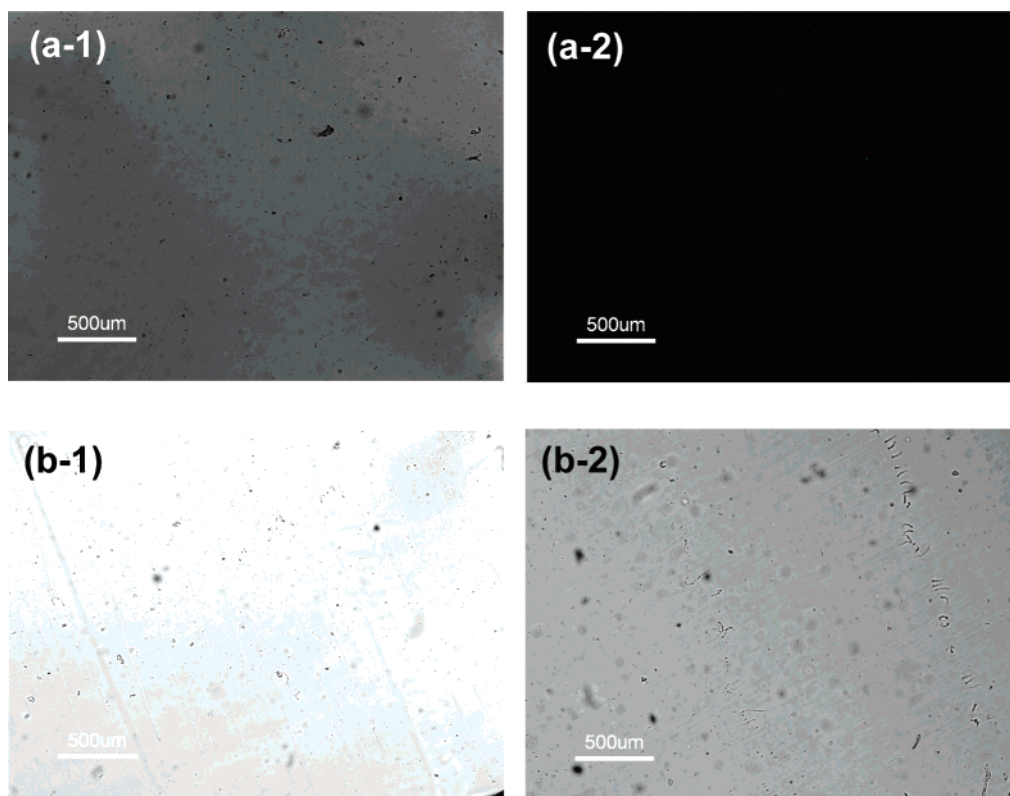


Figure 6. Optical anisotropy of as-prepared and swollen NC gels ($W_{\text{H}_2\text{O}}/W_{\text{dry}}$) measured under crossed polarizers. Δn is the birefringence given by $\Gamma(\text{retardation})/d(\text{thickness})$. (a-1) As-prepared NC12 gel (489 wt %), ($\Delta n = (3 \pm 1) \times 10^{-5}$). (a-2) Swollen NC12 gel (2198 wt %), ($\Delta n \leq 0.3 \times 10^{-5}$). (b-1) As-prepared NC20 gel (377 wt %), ($\Delta n = (48 \pm 8) \times 10^{-5}$). (b-2) Swollen NC20 gel (1092 wt %), ($\Delta n = (10 \pm 3) \times 10^{-5}$).

attached PNIPA chains has an average volume of $d_{\text{clay}}(2) \times (30 + 2\alpha)^2 \text{ nm}^3$, where α is the thickness of the polymer layer at both edges of the clay platelet (Figure 5). When α was assumed to be 1 or 3 nm, $d_{\text{clay}}(2)$ was calculated to be 27.1 or 21.5 nm for NC10 gel and 13.9 nm or 11.0 nm for NC20 gel, and these values correspond to 0.33° or 0.41° and 0.64° or 0.80° , respectively, for 2θ in the XRD (Cu K α) measurements. These results are consistent with the fact that no X-ray diffraction peak corresponding to the inter-clay–platelet distance was observed in the 2θ range above 1.5° for the NC10 and NC20 gels. On the other hand, as shown in a previous paper,²¹ an XRD peak due to the stacking of clay–polymer–clay intercalation was observed when the water content decreased to less than 100 wt % relative to the dried gel. For example, for partially dried NC20 gel with 54 wt % H_2O , $d(\text{XRD})$ was 3.53 nm. For this system, $d_{\text{clay}}(2)$ was calculated to be 3.64 nm using eq 2 with $\alpha = 1$ nm, which is very close to the observed value.

Optical Anisotropy of NC Gels. As previously reported and described above,^{20,21} various properties of NC gels, such as the tensile mechanical properties, the coil-to-globule transition, and the optical anisotropy, changed greatly at the boundary of the critical C_{clay} ($\approx \text{NC10}$). As shown in the former section, we deduced that the aggregation (layer stacking) of clay platelets is spontaneous in as-prepared NC gels with C_{clay} values above the critical value and that this stacking is responsible for the various property changes. Using eq 1, C_{clay}^* was calculated to be $10 (\times 10^{-2} \text{ mol/L } \text{H}_2\text{O})$: NC10 gel), and this result is consistent with those obtained from measurement of both optical and mechanical properties.

Provided that the optical anisotropy of NC gels is mainly due to spontaneous aggregation of clay platelets, this property might be changed by subsequent swelling, since this also dilutes the clay concentration. In fact, as shown in panels a-1 and a-2 of Figure 6, a change in optical anisotropy from anisotropic to

isotropic was observed in NC12 gels which underwent swelling in water at 20°C . The birefringence of as-prepared NC12 gel ($\Delta n = (3 \pm 1) \times 10^{-5}$; Figure 6(a-1)) gradually decreased with increasing swelling, and the swollen NC12 gel with a water content ($W_{\text{H}_2\text{O}}/W_{\text{dry}}$) of 2198 wt % became almost isotropic ($\Delta n \leq 0.3 \times 10^{-5}$; Figure 6(a-2)). Here, $d_{\text{clay}}(1)$ was calculated to be 28.56 nm for the as-prepared NC12 gel and 45.61 nm for the swollen NC12 gel. Since the clay concentration in the latter is much diluted, it may be reasonable for the swollen NC12 gel to become optically isotropic. On the contrary, in the case of NC20 gels, both the as-prepared gel (377 wt %; $\Delta n = (48 \pm 8) \times 10^{-5}$; Figure 6(b-1)) and the swollen one (1092 wt %; $\Delta n = (10 \pm 3) \times 10^{-5}$; Figure 6(b-2)) retained their optical anisotropy, and $d_{\text{clay}}(1)$ was calculated to be 24.25 and 33.50 nm, respectively. Thus, it is concluded that the optical anisotropy in NC gels does not always disappear as a result of increased water content, particularly for NC gels with high C_{clay} values such as NC20 gel. This is probably because the quasi-nematic clay alignment in as-prepared NC gels with high C_{clay} values is hardly disrupted in the swelling process due to the significant clay–polymer–clay interactions. Also, in the case of NC gels with high C_{clay} , the clay platelets during sample preparation might orientate themselves particularly through shear-flowing, and subsequent simple swelling can hardly eradicate the resulting clay alignment. The effect of uniaxial stretching and its accompanying unique change in optical anisotropy for NC gels with different C_{clay} values will be reported in a subsequent paper.

Abnormal Swelling/Deswelling Behavior in NC Gels. As shown above, temperature-induced changes in optical transmittance indicate that NC gels with low C_{clay} values undergo a well-defined coil-to-globule transition, similar to that of linear PNIPA solutions, whereas the transition was gradually depressed

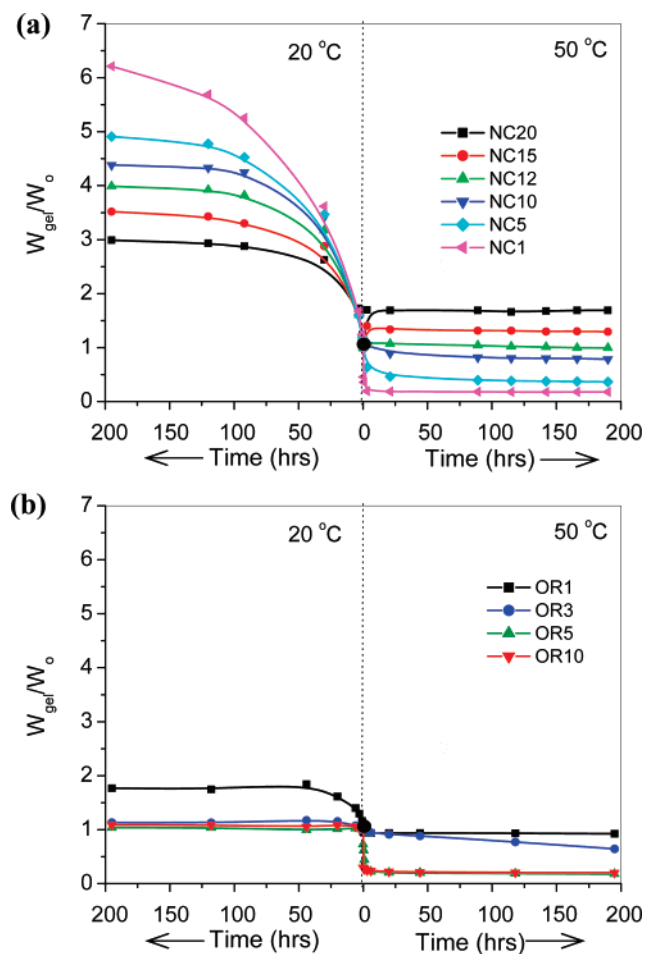


Figure 7. Swelling/deswelling behaviors of (a) NC gels with different C_{clay} and (b) OR gels with different C_{BIS} , measured in water at 20 and 50 °C. Changes in weight ratio (W_{gel}/W_0) with elapsed time are plotted. W_0 is the initial weight of the as-prepared gel (initial size: 5.5 mm diameter \times 30 mm length).

with increasing C_{clay} and entirely disappeared in NC20 gel. It was deduced that, at 50 °C, NC20 gel may still maintain its hydrophilicity, while NC1 gel becomes hydrophobic. These characteristics should also be observed in the swelling/deswelling process.

Parts a and b of Figure 7 show the overall tendencies of swelling and deswelling behaviors of NC and OR gels, respectively, in water at different temperatures, below and above the LCST. Here, the initial gel volume of original (as-prepared) gels was fixed at 712 mm³ (5.5 mm diameter \times 30 mm) for all samples. At 20 °C (<LCST), both NC and OR gels showed the same swelling tendencies; that is, the degree of swelling at specific times changed in almost inverse proportion to each cross-linker concentration (C_{clay} and C_{BIS}). This indicates that the clay platelets act as effective cross-linking agents in NC gels over the whole range of clay content. As for the swelling rate, swelling reached equilibrium within \sim 200 h in NC and OR gels (Figure 7a,b), with the exception of NC1 gel, which took longer to stabilize. On the other hand, at 50 °C (>LCST), NC and OR gels exhibited quite different tendencies. In NC gels, a remarkable change, from a large shrinkage to an expansion, was observed with increasing C_{clay} . In OR gels, an entirely distinct change, from a small shrinkage to a large shrinkage with increasing C_{BIS} , was observed. In the following section, the characteristic swelling and deswelling behavior of NC gels is analyzed and compared with that of OR gels.

Table 1. Degree of Equilibrium Swelling (DES) and Effective Network Density (ν_e) for NC and OR Gels, Calculated Using Eqs 3 and 4, Respectively

hydrogel	NC1	NC5	NC10	NC15	NC20	OR1	OR5
DES	50.94	28.94	22.57	17.61	12.94	16.93	8.55
(W_s/W_{dry})							
ν_e (mol/L)	0.0048	0.0099	0.0127	0.0170	0.0256	0.0431	0.1582

The degree of equilibrium swelling (DES) for NC and OR gels was determined on the basis of the swelling data at 200 h, listed in Table 1. The effective cross-link densities (ν_e) of NC and OR gels were calculated using the DES according to the Flory–Rehner theory.²⁶ Here, an NC gel is a kind of ionic polymer gel containing ionic clay platelets with mobile counterions. The osmotic pressure of an ionic polymer gel can be expressed by eq 3-1.^{27,28} However, in the case of NC gel, the effect of clay on the swelling was totally different from that of conventional organic ionic groups. In NC gels, the swelling decreased with increasing clay concentration, although the usual ionic polymer gel exhibited increased swelling with increasing concentration of ionic groups. This is because the clay platelets act as multifunctional cross-linkers. Therefore, in the present study, we deleted the third contribution, Π_{ion} , to simplify the condition, and used eq 3-2, which relates to nonionic gel systems. Since the osmotic pressure is zero in the equilibrium swelling conditions, eq 4, which corresponds to an affine network model,^{29,30} was used to calculate the effective cross-link density of NC and OR gels.

$$\Pi = \Pi_{\text{mixing}} + \Pi_{\text{elastic}} + \Pi_{\text{ion}}$$

$$\Pi = -\frac{kT}{V_s}[\phi + \ln(1 - \phi) + \chi\phi^2] + \nu_e kT \left[\frac{2}{f} \left(\frac{\phi}{\phi_0} \right) - \left(\frac{\phi}{\phi_0} \right)^{1/3} \right] + \nu^* f^* kT \left(\frac{\phi}{\phi_0} \right) \quad (3-1)$$

$$\Pi = -\frac{kT}{V_s}[\phi + \ln(1 - \phi) + \chi\phi^2] + \nu_e kT \left[\frac{2}{f} \left(\frac{\phi}{\phi_0} \right) - \left(\frac{\phi}{\phi_0} \right)^{1/3} \right] \quad (3-2)$$

where kT is the thermal energy, ν^* is the number of clay platelets per unit volume of NC gel at $\phi = \phi_0$, and f^* is the number of counterions per clay platelet

$$\phi + \ln(1 - \phi) + \chi\phi^2 = -V_s \nu_e \left[\left(\frac{\phi}{\phi_0} \right)^{1/3} - \frac{2}{f} \left(\frac{\phi}{\phi_0} \right) \right] \quad (4)$$

Here, ϕ and ϕ_0 are respectively the network volume fractions at equilibrium swelling and those for the reference state (as-prepared gel). $2/f$ (where f is the functionality) is 0.5 for BIS in OR gels and nearly 0 for clay in NC gels because of its high functionality. V_s is the molar volume of water. $\chi = \chi_1 + \phi\chi_2$, where $\chi_1 = (\Delta H - T\Delta S)/k_B T$, $\chi_2 = 0.518$, $\Delta H = -12.462 \times 10^{-21}$ J, and $\Delta S = -4.717 \times 10^{-23}$ J/K.²⁹ k_B is Boltzmann's constant. The calculated ν_e values for NC and OR gels are listed in Table 1. Analogous to the influence of C_{BIS} in OR gels, ν_e for NC gels increased with increasing C_{clay} , which indicates that, in NC gels, the network is formed by clay as the cross-linker and is stable in water. The fact that values of ν_e for NC gels are generally smaller than those of OR gels is consistent with the observed mechanical properties.

On the other hand, at 50 °C (>LCST), NC1 gel exhibited very rapid deswelling, as previously reported.^{17,18a} The deswelling rate of NC gels gradually decreased with increasing C_{clay} . Also, the volume of deswollen gels gradually increased with

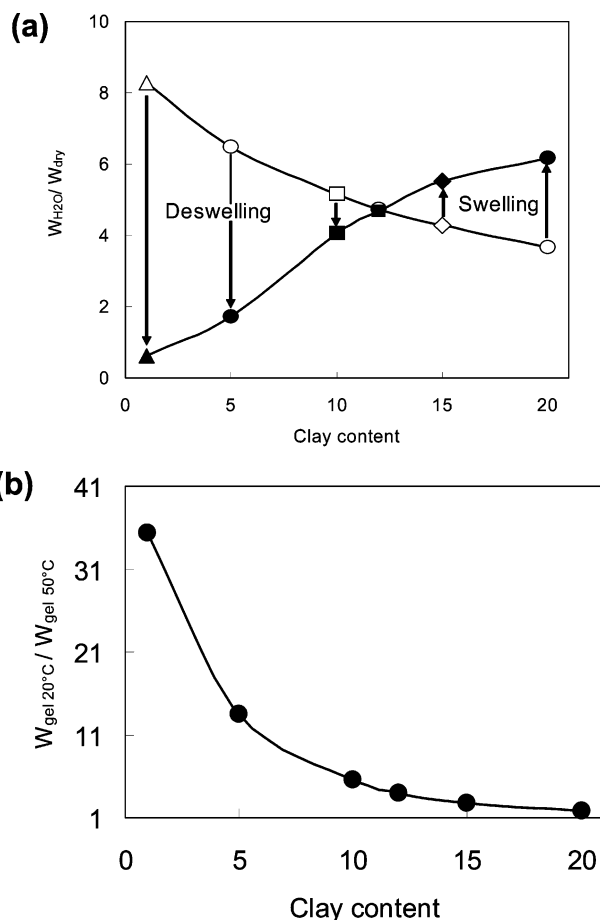


Figure 8. (a) Changes in water content, W_{H_2O}/W_{dry} , for NC gels with different C_{clay} induced by submersing in water at 50 °C. Both deswelling and swelling were observed at 50 °C depending on C_{clay} . (b) Effect of C_{clay} on the ratio of the equilibrium gel weights at 20 °C to those at 50 °C for NC gels.

increasing C_{clay} . So, in NC12 gel, deswelling was completely suppressed and no volume contraction was observed; moreover, NC20 gel simply swelled even at 50 °C (Figure 7a). Thus, it was concluded that incorporation of hydrophilic clay nanoparticles causes a dramatic change in the deswelling property of NC gels. The remarkable change from deswelling to swelling depending on the C_{clay} is summarized in Figure 8a. In the present case, NC12 gel (clay/PNIPA = 0.336 (v/v); 83 wt % H_2O relative to the total gel) exhibited neither swelling nor deswelling when kept at 50 °C. Above NC12, the as-prepared NC gels tended to absorb more water with increasing C_{clay} . For example, NC20 gel (clay/PNIPA = 0.560 (v/v); 79 wt % H_2O), consisting of a considerable amount of hydrophilic clay which seriously restricted the transition of PNIPA chains to their hydrophobic state, behaved like a simple hydrophilic polymeric hydrogel. Therefore, as shown in Figure 8b, the ratio of the gel volumes at 20 and 50 °C decreased rapidly with increasing C_{clay} , sharply at low C_{clay} , e.g., NC1–NC5, and less rapidly at high C_{clay} . Consequently, the volume ratio approached 1 in NC20 or higher- C_{clay} gels, which indicates that the gel volume would be almost constant in water, independent of temperature.

Figure 9 shows changes in gel volume, represented by $W_{gel}(t)/W_{50}(48)$, in repeated runs with the temperature alternating between 20 and 50 °C for NC gels with different C_{clay} . Here, $W_{gel}(t)$ and $W_{gel}^{50}(48)$ are the weights of gel at time t and after submersion for the initial 48 h at 50 °C (=0 h in Figure 9), respectively, for each sample. It was clearly demonstrated that NC1 gel underwent a large and reversible swelling and

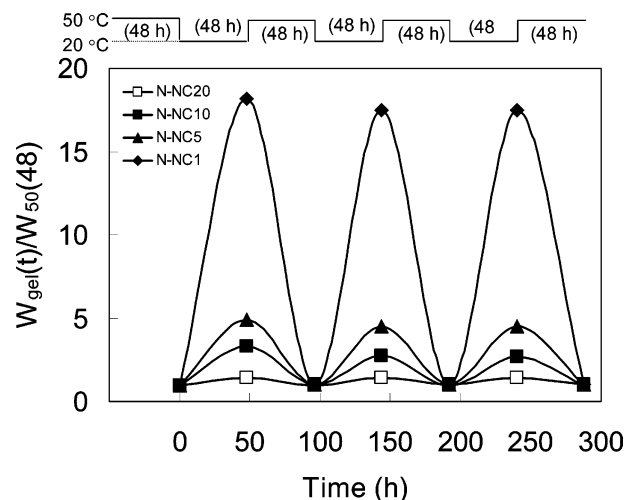


Figure 9. Swelling/deswelling behavior induced by alternating the temperature between 50 and 20 °C for NC1, NC5, NC10, and NC20 gels. The time dependencies of the swelling ratio were calculated using $W_{gel}(t)/W_{50}(48)$. Here, $W_{50}(48)$ is the weight of gel after submersion for the first 48 h at 50 °C.

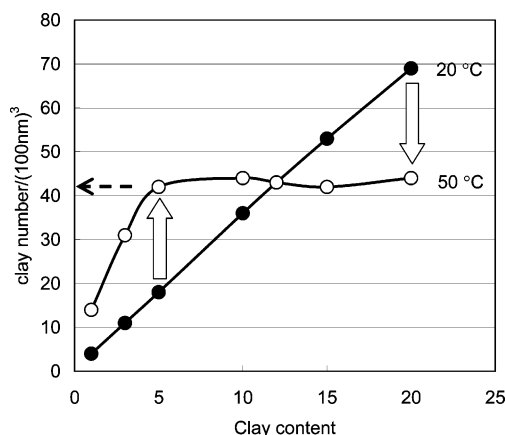


Figure 10. C_{clay} dependencies of the number of clay platelets per unit of gel volume, $(100\ nm)^3$, calculated for as-prepared NC gels at 20 °C and for corresponding shrunk NC gels at 50 °C.

deswelling. With increasing C_{clay} , the gel volume ratio gradually decreased, and NC20 gel hardly exhibited any volume change in either stage. Thus, it was concluded that, in NC gels, thermoresponsive volume change can be controlled to a large extent by varying C_{clay} and that in all cases the changes are reversible and highly reproducible in repeated runs.

Finally, Figure 10 shows the number of clay platelets per unit of gel volume (N_{clay}^*) in as-prepared NC gels (filled circles) and in gels kept at 50 °C (open circles). N_{clay}^* at 50 °C changed in different ways according to the deswelling/swelling behavior; i.e., N_{clay}^* increased in gels with clay concentrations below that for NC12 and decreased in those with clay concentrations above that for NC12. It is interesting to note that N_{clay}^* is almost the same (≈ 42 per $10^6\ nm^3$ of gel) for all NC gels kept at 50 °C, except for NC gels with very low C_{clay} . This indicates that the increase in N_{clay}^* due to the gel contraction has an upper limit of 42; i.e., further increase in clay density is difficult to achieve through deswelling. Also, NC gels with higher clay loading in the as-prepared state, such as NC15 and NC20 gels, tended to expand at 50 °C until they reached the same N_{clay}^* value.

Conclusions

We investigated the highly tunable optical and swelling/deswelling properties associated with the coil-to-globule transi-

tion of PNIPA in NC gels over a broad range of clay contents. The following significant facts were found.

(1) The transmittance change (decrease) induced by altering the temperature varied to a great extent in NC gels, both in magnitude (reduced) and in temperature (shifted to a temperature higher than the normal LCST ($\approx 34^\circ\text{C}$)), probably due to restrictions of the thermal molecular motions of PNIPA chains attached to the hydrophilic clay surfaces or in their proximity. The critical C_{clay} , above which NC gels hardly exhibit any decrease in transmittance, was observed to be $10 \times 10^{-2} \text{ mol/L H}_2\text{O}$ (NC10).

(2) On the assumption of a uniform and random dispersion of the exfoliated clay, the average inter-clay-platelet distance, $d_{\text{clay}}(1)$, and critical C_{clay} , C^*_{clay} , above which the spontaneous aggregation (layer stacking) of clay platelets occurs, were calculated. The calculated C^*_{clay} ($=10 \times 10^{-2} \text{ mol/L H}_2\text{O}$) was consistent with that obtained on the basis of experimental results such as changes in the tensile mechanical properties of strength and modulus, the appearance of optical anisotropy and changes in transmittance (described in (1)). Also, the inter-clay-platelet distance, $d_{\text{clay}}(2)$, calculated assuming the unidirectional alignment of the clay platelets, was consistent with XRD observations for various NC gels, including one partially dried.

(3) Optical anisotropy was observed in NC gels with C_{clay} above a critical value (≈ 10) and was primarily a consequence of the aggregation (layer stacking) of the clay platelets. Also, in NC gels with C_{clay} close to C^*_{clay} , the optical anisotropy could be changed reversibly from anisotropic to isotropic by altering the water content.

(4) NC gels exhibited abnormal swelling/deswelling behaviors depending strongly on C_{clay} . With increasing C_{clay} , swelling ($< \text{LCST}$) and deswelling ($> \text{LCST}$) were both depressed. Furthermore, NC gels with clay contents above that for NC12 did not deswell but swelled even above the normal LCST. Consequently, the ratio of gel volume at 20°C to that at 50°C decreased rapidly and approached 1 with increasing C_{clay} . When keeping NC gels ($> \text{NC3}$) at 50°C , the number of clay platelets per unit of gel volume (N^*_{clay}) was boosted to the same value, $42/(100 \text{ nm})^3$, despite the swelling/deswelling behavior.

Acknowledgment. This work was partially supported by NEDO, Japan.

References and Notes

- (1) Heskins, M.; Guillet, J. E. *J. Macromol. Sci., Chem.* **1968**, *A2*, 1441–1455.
- (2) (a) Otake, K.; Inomata, H.; Konno, M.; Saito, S. *Macromolecules* **1990**, *23*, 283–289. (b) Feil, H.; Bae, Y. H.; Feijen, J.; Kim, S. W. *Macromolecules* **1993**, *26*, 2496–2500. (c) Shibayama, M.; Mizutani, S.; Nomura, S. *Macromolecules* **1996**, *29*, 2019–2024. (d) Li, Y.; Tanaka, T. *J. Chem. Phys.* **1989**, *90*, 5161–5166. (e) Hu, T.; You, Y.; Pan, C.; Wu, C. *J. Phys. Chem. B* **2002**, *106*, 6659–6662. (f) Katsumoto, Y.; Tanaka, T.; Sato, H.; Ozaki, Y. *J. Phys. Chem. A* **2002**, *106*, 3429–3435. (g) Rice, C. V. *Biomacromolecules* **2006**, *7*, 2923–2925.
- (3) (a) Cho, E. C.; Lee, J.; Cho, K. *Macromolecules* **2003**, *36*, 9929–9934. (b) Ding, Y.; Zhang, G. *Macromolecules* **2006**, *39*, 9654–9657.
- (4) (a) Hirokawa, Y.; Tanaka, T. *J. Chem. Phys.* **1984**, *81*, 6379–6380. (b) Hirose, Y.; Amiya, T.; Hirokawa, Y.; Tanaka, T. *Macromolecules* **1987**, *20*, 1342–1344. (c) Matsuo, E. S.; Tanaka, T. *J. Chem. Phys.* **1988**, *89*, 1695–1703. (d) Bae, Y. H.; Okano, T.; Kim, S. W. *J. Polym. Sci., Part B: Polym. Phys.* **1990**, *28*, 923–926.
- (5) Dhara, D.; Chatterji, P. R. *Polymer* **2000**, *41*, 6133–6143.
- (6) Xulu, P. M.; Filipcsei, G.; Zrinyi, M. *Macromolecules* **2000**, *33*, 1716–1719.
- (7) (a) Kato, E. *J. Chem. Phys.* **1997**, *106*, 3792–3797. (b) Takigawa, T.; Araki, H.; Takahashi, K.; Masuda, T. *J. Chem. Phys.* **2000**, *113*, 7640–7645.
- (8) Inomata, H.; Goto, S.; Otake, K.; Saito, S. *Langmuir* **1992**, *8*, 687–690.
- (9) (a) Bae, Y. H.; Okano, T.; Hsu, R.; Kim, S. W. *Macromol. Chem., Rapid Commun.* **1987**, *8*, 481–485. (b) Kataoka, K.; Miyazaki, H.; Bunya, M.; Okano, T.; Sakurai, Y. *J. Am. Chem. Soc.* **1998**, *120*, 12694–12695. (c) Matsumoto, A.; Yoshida, R.; Kataoka, K. *Biomacromolecules* **2004**, *5*, 1038–1045.
- (10) Hu, Z.; Zhang, X.; Li, Y. *Science* **1995**, *269*, 525–527.
- (11) (a) Hellweg, T.; Dewhurst, C. D.; Bruckner, E.; Kratz, K.; Eimer, W. *Colloid Polym. Sci.* **2000**, *278*, 972–978. (b) Hu, Z.; Lu, X.; Gao, J. *Adv. Mater.* **2001**, *13*, 1708–1712. (c) Takeoka, Y.; Watanabe, M. *Adv. Mater.* **2003**, *15*, 199–201.
- (12) (a) Champ, S.; Xue, W.; Huglin, M. B. *Macromol. Chem. Phys.* **2000**, *201*, 931–940. (b) Cai, W.; Anderson, E. C.; Gupta, R. B. *Ind. Eng. Chem. Res.* **2001**, *40*, 2283–2288.
- (13) (a) Okano, T.; Yamada, N.; Sakai, H.; Sakurai, Y. *J. Biomed. Mater. Res.* **1993**, *27*, 1243–1251. (b) Stile, R. A.; Burghardt, W. R.; Healy, K. E. *Macromolecules* **1999**, *32*, 7370–7379. (c) Yamato, M.; Okano, T. *Mater. Today* **2004**, *7*, 42–47.
- (14) (a) Iizawa, T.; Matsuno, N.; Takeuchi, M.; Matsuda, F. *Polym. J.* **1999**, *31*, 1277–1280. (b) Ebara, M.; Aoyagi, T.; Sakai, K.; Okano, T. *J. Polym. Sci., Part A: Polym. Chem.* **2001**, *39*, 335–342.
- (15) (a) Yoshida, R.; Uchida, K.; Kaneko, Y.; Sakai, K.; Kikuchi, A.; Sakurai, Y.; Okano, T. *Nature (London)* **1995**, *374*, 240–242. (b) Kaneko, Y.; Nakamura, S.; Sakai, K.; Kikuchi, A.; Aoyagi, T.; Sakurai, Y.; Okano, T. *J. Biomater. Sci., Polym. Ed.* **1999**, *10*, 1079–1091. (c) Okajima, T.; Harada, I.; Nishio, K.; Hirotsu, S. *Jpn. J. Appl. Phys.* **2000**, *39*, L875–L877. (d) Zhang, X.-Z.; Zhuo, R.-X. *Langmuir* **2000**, *17*, 12–16. (e) Serizawa, T.; Wakita, K.; Akashi, M. *Macromolecules* **2002**, *35*, 10–12.
- (16) (a) Messersmith, P. B.; Znidarsich, F. *Mater. Res. Soc. Symp. Proc.* **1997**, *457*, 507–512. (b) Liang, L.; Liu, J.; Gong, X. *Langmuir* **2000**, *16*, 9895–9899.
- (17) Haraguchi, K.; Takehisa, T. *Adv. Mater.* **2002**, *14*, 1120–1124.
- (18) (a) Haraguchi, K.; Takehisa, T.; Fan, S. *Macromolecules* **2002**, *35*, 10162–10171. (b) Haraguchi, K.; Farnworth, R.; Ohbayashi, A.; Takehisa, T. *Macromolecules* **2003**, *36*, 5732–5741.
- (19) (a) Haraguchi, K.; Li, H. J.; Matsuda, K.; Takehisa, T.; Elliott, E. *Macromolecules* **2005**, *38*, 3482–3490. (b) Shibayama, H.; Karino, T.; Miyazaki, S.; Okabe, S.; Takehisa, T.; Haraguchi, K. *Macromolecules* **2005**, *38*, 10772–10781. (c) Miyazaki, S.; Karino, T.; Endo, H.; Haraguchi, K.; Shibayama, M. *Macromolecules* **2006**, *39*, 8112–8120.
- (20) Haraguchi, K.; Li, H. J. *Angew. Chem., Int. Ed.* **2005**, *44*, 6500–6504.
- (21) Haraguchi, K.; Li, H. J. *Macromolecules* **2006**, *39*, 1898–1905.
- (22) (a) Avery, R. G.; Ramsay, J. D. F. *J. Colloid Interface Sci.* **1986**, *109*, 448–454. (b) Mourchid, A.; Delville, A.; Lambard, J.; Lecolier, E.; Levitz, P. *Langmuir* **1995**, *11*, 1942–1950. (c) Ruzicka, B.; Zulian, L.; Ruocco, G. *Phys. Rev. Lett.* **2004**, *93*, 258301.
- (23) *Clay Handbook: The Clay Science Society of Japan*; Gihodo: Tokyo, 1987.
- (24) Schild, H. D. *Prog. Polym. Sci.* **1992**, *17*, 163–249.
- (25) Murata, K.; Haraguchi, K. *J. Mater. Chem.* **2007**, *17*, 3385–3388.
- (26) Flory, P. J.; Rehner, J., Jr. *J. Chem. Phys.* **1943**, *11*, 521–526.
- (27) Tanaka, T.; Fillmore, D.; Sun, S.-T.; Nishio, I. *Phys. Rev. Lett.* **1980**, *45*, 1636–1639.
- (28) Hirotsu, S.; Hirokawa, Y.; Tanaka, T. *J. Chem. Phys.* **1987**, *87*, 1392–1395.
- (29) (a) Baker, J. P.; Hong, L. H.; Blanch, H. W.; Prausnitz, J. M. *Macromolecules* **1994**, *27*, 1446–1454. (b) Shibayama, M.; Shirotani, Y.; Hirose, H.; Nomura, S. *Macromolecules* **1997**, *30*, 7307–7312.
- (30) Hirotsu, S. *J. Chem. Phys.* **1991**, *94*, 3949–3957.

MA071348I